Eur J Nucl Med Mol Imaging (2012) 39:1977–1995
DOI 10.1007/s00259-012-2215-8

GUIDELINES

# EANM 2012 guidelines for radionuclide imaging of phaeochromocytoma and paraganglioma

**David Taïeb · Henri J. Timmers · Elif Hindié · Benjamin A. Guillet · Hartmut P. Neumann · Martin K. Walz · Giuseppe Opocher · Wouter W. de Herder · Carsten C. Boedeker · Ronald R. de Krijger · Arturo Chiti · Adil Al-Nahhas · Karel Pacak · Domenico Rubello**

Published online: 28 August 2012


**Abstract**
*Purpose* Radionuclide imaging of phaeochromocytomas (PCCs) and paragangliomas (PGLs) involves various functional imaging techniques and approaches for accurate diagnosis, staging and tumour characterization. The purpose of the present guidelines is to assist nuclear medicine practitioners in performing, interpreting and reporting the results of the currently available SPECT and PET imaging approaches. These guidelines are intended to present information specifically adapted to European practice.
*Methods* Guidelines from related fields, issued by the European Association of Nuclear Medicine and the Society of Nuclear Medicine, were taken into consideration and are partially integrated within this text. The same was applied to the

**Purpose** The purpose of these guidelines is to assist nuclear medicine practitioners in:
1. Understanding the role and challenges of radionuclide imaging of phaeochromocytomas/paragangliomas.
2. Providing practical information for performing different imaging procedures for these tumours.
3. Providing an algorithm for selecting the most appropriate imaging procedure in each specific clinical situation to localize and characterize these tumours.

D. Taïeb (✉)
Department of Nuclear Medicine, La Timone University Hospital, CERIMED,
Aix-Marseille University, France
e-mail: david.taieb@ap-hm.fr

H. J. Timmers
Department of Endocrinology, Radboud University Nijmegen Medical Centre,
Nijmegen, The Netherlands

E. Hindié
Department of Nuclear Medicine, Haut-Lévêque Hospital, University of Bordeaux-2,
Bordeaux, France

B. A. Guillet
Department of Radiopharmacy, La Timone University Hospital, CERIMED,
Aix-Marseille University, France

H. P. Neumann
Preventive Medicine Unit, Department of Medicine, University Medical Center, Albert-Ludwigs-University,
Freiburg, Germany

M. K. Walz
Department of Surgery and Center of Minimally Invasive Surgery, Kliniken Essen-Mitte,
Essen, Germany

G. Opocher
Endocrinology Unit, Department of Medical and Surgical Sciences, University Hospital of Padova,
Padova, Italy

W. W. de Herder
Department of Internal Medicine, Section Endocrinology, Erasmus MC,
Rotterdam, The Netherlands

C. C. Boedeker
Department of Otorhinolaryngology – Head and Neck Surgery, University of Freiburg,
Freiburg, Germany

relevant literature, and the final result was discussed with leading experts involved in the management of patients with PCC/PGL. The information provided should be viewed in the context of local conditions, laws and regulations.
*Conclusion* Although several radionuclide imaging modalities are considered herein, considerable focus is given to PET imaging which offers high sensitivity targeted molecular imaging approaches.

**Keywords** Guidelines · Review literature · Radionuclide imaging · Paraganglioma · Phaeochromocytoma

## Background information and definitions

### The paraganglion system

Paragangliomas (PGLs) are tumours that develop from neuroendocrine cells derived from pluripotent neural crest stem cells and are associated with neurons of the autonomic nervous system. They may arise anywhere along the paraganglial system and can be associated with the sympathetic or the parasympathetic nervous system. Those associated with the sympathetic nervous system derive from the adrenal medulla, the organ of Zuckerkandl, or other chromaffin cells that may persist beyond embryogenesis, while those associated with the parasympathetic nervous system develop from neural crest cells derivates present in the parasympathetic paraganglia (chemoreceptors) mainly located in the head and neck (H&N). Thus, PGLs can be distributed from the skull base to the sacrum, with a predilection for the following sites: middle ear (glomus tympanicum), the dome of the internal jugular vein (glomus jugulare), at the bifurcation of the common carotid arteries (glomus caroticum, carotid body), along the vagus nerve, in the mediastinum (from the aortopulmonary body or the thoracic sympathetic chain), in the adrenal medulla and in the abdominal and pelvic paraaortic regions. Based on the classification published in 2004 by the World Health Organization, the term phaeochromocytoma (PCC) should be reserved solely for adrenal PGL.

R. R. de Krijger
Department of Pathology, Josephine Nefkens Institute, Erasmus MC, University Medical Center Rotterdam, Rotterdamn, The Netherlands

A. Chiti
Department of Nuclear Medicine, Istituto Clinico Humanitas, Rozzano, MI, Italy

A. Al-Nahhas
Department of Nuclear Medicine, Hammersmith Hospital, London, UK

K. Pacak
Program in Reproductive and Adult Endocrinology, Eunice Kennedy Shriver National Institutes of Child Health and Human Development, National Institutes of Health, Bethesda, MD, USA

D. Rubello (✉)
Department of Nuclear Medicine, PET/CT Centre, Radiology, Neuroradiology, Medical Physics, 'Santa Maria della Misericordia' Hospital, Rovigo, Italy
e-mail: domenico.rubello@libero.it

### Clinical presentation

PCCs/PGLs are rare tumours (annual incidence of 0.1 to 0.6 per 100,000 population). They account for about 4 % of adrenal incidentalomas and their prevalence is higher in autopsy series. PCCs and PGLs of sympathetic chains usually cause symptoms of catecholamine over-secretion (e.g. sustained or paroxysmal elevations in blood pressure, headache, episodic profuse sweating, palpitations, pallor, and apprehension or anxiety). By contrast, H&N PGL and parasympathetic thoracic PGL are almost always (up to 95 %) nonsecreting tumours which are discovered on imaging studies or revealed by symptoms of compression or infiltration of the adjacent structures (e.g. hearing loss, tinnitus, dysphagia, cranial nerve palsies).

### Spectrum of hereditary syndromes

PCCs/PGLs are characterized by a high frequency of hereditary forms (overall 35 %) with a propensity for multifocal disease [1, 2]. They may coexist with other tumour types in multiple neoplasia syndromes. Research in molecular genetics has so far resulted in the identification of ten susceptibility genes for tumours of the entire paraganglial system, including SDHB (succinate dehydrogenase subunit B or complex II of the mitochondrial respiratory chain), SDHC (subunit C), SDHD (subunit D), VHL (Von Hippel-Lindau), RET (REarranged during Transfection) and NF1 (neurofibromatosis type 1), and the very recently reported susceptibility genes SDHAF2 (succinate dehydrogenase complex assembly factor 2, also called SDH5), TMEM127 (transmembrane protein 127), SDHA (subunit A), and MAX (MYC associated factor X). Genotypic analysis can be performed by PCR amplification of DNA isolated from blood samples of patients and test deletions and/or rearrangements of one or several exons, even an entire gene. Some correlations between the gene involved and tumour location have been found (Table 1). Mutations in one of the succinate dehydrogenase subunit genes (collectively SDHx) are each associated with a distinct PGL syndrome and often with a high percentage of extraadrenal locations. Furthermore, PCCs/PGLs with an underlying SDHB mutation are associated with a higher risk of aggressive behaviour, development of metastatic disease and ultimately death. Malignancy

**Table 1** PCC/PGL locations in hereditary syndromes

| Gene | Syndrome name | H&N | Thorax | Adrenal (PCC) | Abdominal extraadrenal | Malignancy risk |
|---|---|---|---|---|---|---|
| SDHA | – | ++ | +/– | + | + | +/– |
| SDHB | PGL4[a] | + | + | + | ++ | ++ |
| SDHC | PGL3[a] | ++++ | +/– | +/– | +/– | +/– |
| SDHD | PGL1[ab] | ++ | + | ++ | ++ | +/– |
| SDHAF2 (SDH5) | PGL2 | ++++ | – | – | – | – |
| RET | MEN2[c] | +/– | – | ++++ | +/– | +/– |
| VHL | VHL[d] | +/– | +/– | ++++ | + | +/– |
| NF1 | NF1[e] | – | – | ++++ | +/– | + |
| TMEM127 | – | + | – | ++++ | + | – |
| MAX | – | – | – | ++++ | + | + |

– never reported, +/– <10 %, + 10–<30 %, ++ 30–<60 %, +++ 60–<90 %, ++++90–100 %

[a] Non-KIT/PDGFRA gastrointestinal stromal tumours may be caused by mutations in the SDHB, SDHC and SDHD genes and be associated with PGL in the Carney-Stratakis syndrome.

[b] SDHD mutation is characterized by maternal imprinting; the disease occurs only when the mutations are inherited from the father. A case of GH-secreting pituitary adenoma has been reported in a kindred with PGL1 syndrome.

[c] Medullary thyroid carcinomas most often reveal the disease.

[d] Von Hippel-Lindau disease is an autosomal dominant disorder, which also predisposes to renal tumours and clear cell carcinoma, pancreatic serous cystadenomas, pancreatic neuroendocrine tumours, and haemangioblastoma of the eye and central nervous system.

[e] NF1 is characterized by the presence of multiple neurofibromas, café-au-lait spots, Lisch nodules of the iris and other rare disorders.

risk of SDHB mutation-associated tumours has been estimated to range from 31 % to 71 %. Immunohistochemical studies might become in a near future a screening method to select patients for subsequent molecular genetic testing.

## Clinical indications for nuclear imaging

### Confirmation of diagnosis of PCC/PGL and other findings

The diagnosis of PCC/PGL is often based on the presence of high levels of plasma or urinary metanephrines. Radiological features of anatomical imaging (CT/MRI) may also be suggestive of the diagnosis. In cases of a nonsecreting adrenal mass, the high specificity of functional imaging may contribute to the diagnosis.

In the presence of a retroperitoneal extraadrenal nonrenal mass, it is important to differentiate a PGL from other tumours or lymph node involvement including metastases. A biopsy is not always contributory or even recommended since it can carry a high risk of hypertensive crisis and tachyarrhythmia, and therefore it should only be done if PGL is ruled out in any patient presenting with symptoms and signs of catecholamine excess. Although specific functional imaging is very helpful to distinguish PCC/PGL from other tumours, it is usually not done before biochemical results are available.

In H&N locations, there are also many differential diagnoses such as lymph node metastasis, neurogenic tumour (schwannoma, neurofibroma, ganglioneuroma), jugular meningioma, internal jugular vein thrombosis, internal carotid artery aneurysm, haemangioma and vascular malposition.

### Staging at initial presentation

Most often, PCCs/PGLs are benign and progress slowly. The rate of metastasization is wide, ranging from less than 1 % to more than 60 %, depending on tumour location, size and genetic background. Functional imaging is probably not necessary in the preoperative work-up of patients meeting the following criteria: >40 years of age, no family history, small (less than 3.0 cm) PCC secreting predominantly metanephrines and negative genetic testing. However, since the genetic status is often not available before surgery, the possibility of multifocal or metastatic disease should be considered, and nuclear imaging may be useful in this regard. In patients without a family history, it is particularly important to exclude multiple lesions in younger patients (≤40 years) and those with SDHD gene mutations and to exclude metastatic lesions in patients with SDHB gene mutations. Malignancy at initial presentation should be highly suspected in patients with a large PCC.

In extraadrenal PGL regardless of its size and/or hereditary syndromes, as well as in identifying metastatic PGL, pretreatment imaging is crucial for providing accurate staging of the disease. In this respect, nuclear imaging plays a leading role. H&N PGLs raise the critical problem of locoregional extension and multifocality. Metastatic forms are rare.

Restaging and follow-up

Nuclear imaging may be used for restaging following completion of treatment of aggressive tumours. It could also localize tumour sites in patients with positive biochemical results or suspicion of disease recurrence. A PASS (Pheochromocytoma of the Adrenal gland Scaled Score) score of ≥4, a large primary tumour and/or a mutation in the SDHB gene should alert the clinician to carry out extended and prolonged (life-long) monitoring.

Selection for targeted radiotherapy

Nuclear imaging gives valuable information when planning targeted radionuclide therapy with radiolabelled MIBG or somatostatin (SST) analogues. Besides confirming uptake, it helps achieve personalized dosimetric evaluation.

Response evaluation

Nuclear imaging might be helpful in assessing metabolic and other tumour responses in metastatic PCC/PGL.

## Clinically useful information for optimal interpretation

The nuclear medicine physician should obtain the following information whenever possible:

1. Personal history for PCC/PGL or other tumours.
2. Personal history of surgery, chemotherapy and radiotherapy (including timing).
3. Genetic mutation or documented family history of PCC/PGL.
4. Results of laboratory tests (metanephrines, methoxytyramine, calcitonin, chromogranin A).
5. Results of previous anatomical and functional imaging modalities, including baseline and nadir on-treatment imaging for the assessment of tumour response(s).
6. Drugs that may interfere with the accuracy of the procedures and measurements.

## General considerations for image acquisition and interpretation

1. PCCs/PGLs have different preferential sites of origin that must be known. The integration of functional and anatomical imaging is very helpful.
2. Images are usually acquired from the top of the skull (for a large jugular PGL) to the bottom of the pelvis. In case of suspicion of recurrent or metastatic disease, whole-body images may be needed.
3. Malignancy is defined only by the presence of metastatic lesions at sites where chromaffin cells are normally absent (i.e. liver, lung, bone).
4. The presence of extraadrenal retroperitoneal PGL and/or multifocal tumours increases the chance of hereditary syndrome and an extensive search for additional PCCs/PGLs and any other syndromic lesions (e.g. gastrointestinal stromal tumour, renal cell carcinoma, pancreatic tumour, haemangioblastoma, medullary thyroid carcinoma (MTC), or pituitary tumours) is required.
5. All nonphysiological and suspicious foci of tracer uptake must be described since PGL may arise in various atypical locations (e.g., orbital, intrathyroidal, hypoglossal, cardiac, pericardial, gallbladder, cauda equina).
6. Metastases from PCC/PGL are often small and numerous and could be difficult to precisely localize on coregistered CT images of combined SPECT and PET/CT (unenhanced procedure, thick anatomical sections, shift between CT and PET images).

## Reporting

The report to the referring physician should describe:

1. The clinical setting, a summary of results of previous imaging, and the clinical question that is raised.
2. The procedure: radiopharmaceutical, activity administered, acquisition protocol, CT parameters in case of hybrid imaging and patient radiation exposure.
3. The positive findings and interpretation for each level (i.e., H&N, chest, abdomen and pelvis, bone/bone marrow)
4. Comparative data analysis with other imaging studies or previous nuclear imaging.
5. Conclusion: if possible, a clear diagnosis should be made accompanied, when appropriate, by a description of the study limitations. When conclusive evidence requires additional diagnostic functional or morphological examinations or an adequate follow-up, a request for these follow-up examinations should be included in the report.

SPECT and PET imaging protocols

Conventional $^{123}$I-MIBG SPECT and $^{111}$In-pentetreotide SPECT are well-established nuclear imaging modalities in the staging and restaging of PCC/PGL. Also, SPECT/CT has now become more widely available and has the advantage of simultaneous acquisition of both morphological and functional data, thus increasing diagnostic confidence in image interpretation and enhancing sensitivity. However,

these conventional examinations are associated with some practical constraints such as long imaging times, gastrointestinal tract artefacts requiring bowel cleansing in some patients, thyroid blockage and the need for withdrawal of certain medications that interfere with interpretation. The somewhat low resolution of conventional SPECT imaging might limit the ability to detect tiny lesions. SPECT also does not provide a quantifiable estimate of tumour metabolism (tracer uptake). Thus, the use of PET imaging has been growing rapidly in the imaging of PGLs, paralleled by a great effort towards the development of new highly sensitive tracers. $^{18}$F-FDG is the most accessible tracer and is playing an increasingly important role in PCC/PGL imaging. $^{18}$F-FDOPA is also available from different pharmaceutical suppliers. Other tracers, such as $^{18}$F-FDA (fluorodopamine) or $^{11}$C-HED (meta-hydroxephedrine) are also very specific and useful for localization of PCC/PGL, but are presently available at only a few centres. $^{68}$Ga-conjugated peptides are still in the evaluation stage and are used in the setting of clinical trials, although $^{68}$Ga-conjugated peptides are currently used in many centres for clinical purposes.

## $^{123}$I-Iobenguane/$^{123}$I-metaiodobenzylguanidine scintigraphy

### Radiopharmaceutical

MIBG is commercially available labelled with $^{123}$I or $^{131}$I. $^{123}$I-MIBG scintigraphy is preferable to $^{131}$I-MIBG scintigraphy because (a) it provides images of higher quality (the 159 keV emission of $^{123}$I can be detected better with conventional gamma cameras), (b) the lower radiation burden of $^{123}$I allows a higher permissible administered activity, resulting in a higher count rate, (c) SPECT can more feasibly be performed with $^{123}$I, and (d) with $^{123}$I-MIBG scintigraphy there is less time between injection and imaging (24 h) than with $^{131}$I-MIBG scintigraphy (48–72 h). Nevertheless, $^{123}$I-MIBG might not be available in every nuclear medicine facility. Although $^{131}$I-MIBG can be used in such circumstances, it is not recommended because of low sensitivity and unfavourable dosimetry.

### Mechanism of cellular uptake

MIBG, an iodinated analogue of guanidine, is structurally similar to norepinephrine (NE). Guanidine analogues have the same transport pathway as NE via the cell membrane NE transporter (NET). A nonspecific uptake has also been reported for MIBG uptake in PCC/PGL tissues [3, 4]. In the cytoplasmic compartment, MIBG is stored in the neurosecretory granules via vesicular monoamine transporters 1 and 2 (VMAT 1 and 2). This vesicular uptake is predominant in PCCs/PGLs [5] and remains in the cytoplasm in neuroblastoma. MIBG specifically concentrates in tissues expressing NET, allowing specific detection of other neuroendocrine tumours and to some degree the adrenal medulla.

### Pharmacokinetics

After intravenous administration, MIBG concentrates in the liver (33 %), lungs (3 %), heart (0.8 %), spleen (0.6 %) and salivary glands (0.4 %). In the vascular compartment, the small amount of remaining MIBG concentrates in platelets through the 5HT transporter. Tracer uptake in normal adrenal glands is weak; normal adrenals can be faintly visible. The majority of MIBG is excreted unaltered by the kidneys (60–90 % of the injected dose is recovered in the urine within 4 days; 50 % within 24 h), faecal elimination is weak (<2 % up to day 4). In patients with PCC/PGL, uptake in the heart and liver is significantly lowered by about 40 % [6].

### Synthesis and quality control

MIBG labelled with $^{123}$I or $^{131}$I is currently commercially available in a “ready to use” formulation and conforms to the criteria laid down in the European Pharmacopoeia. The labelled product is available in a sterile solution for intravenous use. The solution is colourless or slightly yellow, contains 0.15–0.5 mg/ml of MIBG, is stable for 60 h after synthesis and can be diluted in sterile water or saline. The activity of MIBG should be measured in a calibrated ionization chamber, and radiochemical purity can be determined using thin-layer chromatography.

### Drug interactions

Many drugs modify the uptake and storage of MIBG and may interfere with MIBG imaging [7]. For a review of drugs that may interact or interfere with MIBG uptake, the reader can refer to some previous reviews and guidelines [8, 9]. These include opioids, tricyclic antidepressants, sympathomimetics, antipsychotics and antihypertensive agents [8, 9]. Labetalol, for example, has been reported to cause false-negative scans and must be stopped 10 days prior to MIBG administration [10, 11]. A single oral dose of amitriptyline, a tricyclic antidepressant, enhances cardiac MIBG washout [12]. A post-therapy MIBG scan failed to detect the vast majority of metastatic PCC/PGL lesions in a polytoxicomanic patient in whom the diagnostic scan was positive [13]. Nifedipine, on the other hand, can cause prolonged retention of the tracer in PCCs/PGLs [14]. Very high serum catecholamines levels may be associated with lower MIBG accumulation [15–18]. To date, many of these interactions are suspected on the basis of

in vitro/preclinical observations or only expected on the basis of their pharmacological properties, and thus should be interpreted with caution. Furthermore, mechanisms involved in MIBG uptake or retention may differ between models. For example, specific uptake of MIBG is mediated by 5HT transporters in platelets and by NET in PCC/PGL.

Side effects

- Rare adverse events (tachycardia, pallor, vomiting, abdominal pain) that can be minimized by slow injection.
- No adverse allergic reactions.

Recommended activity

The recommended activities in adults are 40–80 MBq for $^{131}$I-MIBG, and 200–400 MBq for $^{123}$I-MIBG. The activity administered to children should be calculated on the basis of a reference dose for an adult, scaled to body weight according to the schedule proposed by the EANM Paediatric Task Group ($^{123}$I-MIBG 80–400 MBq).

Administration

Intravenous injection. Slow injection is recommended (over at least 5 min).

Radiation dosimetry

Dosimetry can be obtained from the ICRP tables. The effective doses are 0.013 mSv/MBq for $^{123}$I-MIBG and 0.14 mSv/MBq for $^{131}$I-MIBG in adults, and 0.037 mSv/MBq for $^{123}$I-MIBG and 0.43 mSv/MBq for $^{131}$I-MIBG in children (5-year old). There is an increased radiation dose from CT in SPECT/CT protocols (volume CT dose index: 3–5 mGy depending on acquisition parameters).

Pregnancy

Clinical decision is necessary to consider the benefits against the possible harm of carrying out any procedure in patients known or suspected to be pregnant.

Breast feeding

Breast feeding should be discontinued for at least 2 days after scintigraphy using $^{123}$I-MIBG and stopped completely if $^{131}$I-MIBG is used.

Renal insufficiency

Plasma clearance of $^{123}$I-MIBG is reduced in patients with renal insufficiency. $^{123}$I-MIBG is not cleared by dialysis [19].

Patient preparation

- Thyroid blockade (130 mg/day of potassium iodide; equivalent to 100 mg of iodine) should be started 1 day before tracer injection and continued for 2 days for $^{123}$I-MIBG and 5 days for 131-MIBG. Potassium perchlorate may be substituted for iodine in iodine-allergic patients and started 4 h before tracer injection and continued for 2 days (400–600 mg/day).
- Drugs interfering with MIBG uptake and retention should be discontinued. All but labetalol have to be withheld for 1–3 days, depending on the medication, with the exception of depot forms of antipsychotics, for which the withdrawal period suggested is 1 month. The decision should be weighed in the context of the clinical setting.

Image acquisition and reconstruction

- $^{123}$I-MIBG scans are usually obtained 20 to 24 h after tracer injection.
- Imaging field

  Anterior and posterior planar static images of the H&N (+ right and left lateral views), thorax, abdomen and pelvis are obtained for 10–15 min per image (using a 256×256 matrix, with a large-field-of-view camera, a low-energy collimator, and a 20 % window centred at the 159 keV photopeak). Many centres prefer medium-energy collimators because they reduce septal penetration of high-energy photons that are part of the $^{123}$I decay scheme.
- Optional images
  - The imaging session may be completed with a SPECT (SPECT/CT) scan over the anatomical regions showing pathological tracer uptake on planar images. The SPECT images are obtained over a 360° orbit (128×128 word matrix, 6° angle steps, 30–45 s per stop). Coregistered CT images (100–130 kV, mAs modulation recommended) from SPECT/CT cameras enable attenuation and facilitate precise localization of any focus of increased tracer. Some authors consider that SPECT or SPECT/CT should be regarded as a mandatory part of the study.
  - Early static images at 4 to 6 h after injection.
  - Planar whole-body imaging can also be performed. For whole-body images, anterior and posterior images are acquired into 1,024×512 word or 1,024×256 word matrix for a minimum of 30 min (maximum speed 6 cm/min).
- Reconstruction

  SPECT iterative reconstruction or reconstruction

using another validated protocol that allows accurate visualization of lesions (to be adapted to the clinical setting), and CT-based attenuation correction for SPECT/CT, can also be performed. Attenuation correction can be performed on SPECT images alone based on the constant μ before or after processing (e.g. Sorenson, Chang), but it is not usually done. Scatter correction methods using spectral analysis can be used to improve the accuracy of quantification.

Image processing

- Visual analysis

  Physiological distribution: Normal uptake of $^{123}$I-MIBG can be observed in the myocardium, salivary glands, thyroid gland (if no adequate thyroid blockade is performed), liver, lungs, adrenal glands (slight uptake can be seen in up to 80 % of patients) and bowel. The large intestine may also be visible. Uptake in brown adipose tissue should be considered as a normal distribution of MIBG, although this may be more common in children than in adults.

  Pathological uptake: $^{123}$I-MIBG uptake in the adrenal glands is considered normal if mild (less than or equal to liver uptake) or symmetrical and when the glands are not enlarged on the CT scan. High-intensity adrenal uptake (more intense than liver uptake) or inhomogeneous adrenal uptake is abnormal with a concordant enlarged gland. Extraadrenal sites of uptake that cannot be explained by normal physiological distribution are considered abnormal. Precise SPECT/CT localization can be of help in the final diagnosis.
- Quantification

  The simplest and most reproducible methodology is to quantify adrenal uptake on the 24-h planar images. SPECT/CT offers the potential for quantification, but requires further studies.

Pitfalls

- False-positives

  CT-based attenuation correction often leads to enhanced physiological visualization of the adrenal medulla and may therefore lead to false-positive interpretation. In patients with MEN2, $^{123}$I-MIBG scintigraphy is of limited value for discriminating physiological uptake from mild adrenal medulla hyperplasia or small PCC. False-positive results have also been related to tracer uptake by other neuroendocrine lesions (carcinoid tumour, MTC, Merkel cell carcinoma, ganglioneuroma). Rarely, MIBG uptake has been reported in adrenocortical adenoma or carcinoma, retroperitoneal angiomyolipoma and haemangioma. SPECT/CT may avoid misleading accumulations in the liver (inhomogeneous uptake, hepatic haemangioma, hepatocellular carcinoma), in the renal parenchyma (diffuse for renal artery stenosis, focal for acute pyelonephritis) or in the urinary tract (hydronephrosis, renal cysts).
- False-negatives

  H&N PGL, retroperitoneal extraadrenal PGL, SDHB-related tumours, small lesions, large PCC/PGL with substantial necrosis or haemorrhage, poorly differentiated tumours (low expression of VMAT-1) are more prone to yield false-negative results [20–24]. False-negative results may also result from drug interferences.

Diagnostic accuracy

$^{123}$I-MIBG scintigraphy has a sensitivity ranging from 83 % to 100 % and a high specificity (95–100 %) for PCC. Its specificity decreases in MEN2-related PCC. Studies that have included high numbers of extraadrenal, multiple or hereditary PGLs have shown reduced sensitivity of $^{123}$I-MIBG scintigraphy (52–75 %) [20–23]. $^{123}$I-MIBG scintigraphy may be suboptimal in patients with special genotypic features such as in VHL and SDHB-related PGLs [24–26]. In patients with metastatic disease, $^{123}$I-MIBG scintigraphy may lead to a significant underestimation of the extent of disease with potentially inappropriate management. $^{123}$I-MIBG scintigraphy may also select candidates for $^{131}$I-MIBG therapy. The sensitivity of $^{123}$I-MIBG scintigraphy is low in H&N PGLs (18–50 %).

## $^{111}$In-Pentetreotide scintigraphy

Radiopharmaceutical

$^{111}$In-Pentetreotide is a [$^{111}$In-DTPA$^{0}$] conjugate of octreotide, a long-acting SST analogue.

Mechanism of uptake

$^{111}$In-Pentetreotide specifically binds to SST receptors (SSTR) expressed on cell membranes, especially subtypes 2 and 5 (SST4 and SST5). SSTR are expressed on many cells of neuroendocrine origin, and therefore in tumours derives from these cell types.

Pharmacokinetics

By 24 h after intravenous administration, $^{111}$In-pentetreotide has cleared from the blood, almost entirely through the kidneys (50 % of the injected dose is recovered in the urine by 6 h, 85 % within 24 h). Some of the tracer is, however, retained in tubular cells. Hepatobiliary excretion and spleen trapping are, respectively, 2 % and 2.5 % of the administered dose. The pituitary and thyroid glands can also be visualized [27, 28].

Synthesis and quality control

$^{111}$In-Pentetreotide is commercially available (Octreoscan®, Covidien) and is supplied as a single-dose kit for radiolabelling. The kit contains two sterile vials containing lyophilized pentetreotide (10 μg) and indium chloride (122 MBq/1.1 ml at room temperature). The radiopharmaceutical is prepared by adding to the vial containing pentetreotide the desired activity of $^{111}$In-indium chloride at room temperature. The preparation should be used within 6 h and can be diluted in sterile saline (2–3 ml). The preparation of the $^{111}$In-pentetreotide is stable for 6 h, and should not be used if radiochemical purity is less than 98 %. The pH of the solution ranges between 3.8 and 4.3. Instant thin-layer chromatography can be used to check radiochemical purity with 0.1 N sodium citrate adjusted with HCl to pH 5 as the mobile-phase (Rf values: $^{111}$In-pentetreotide 0.0, unbound $^{111}$In 1.0).

Drug interactions and side effects

The amount of pentetreotide injected is about 10 μg and is not expected to have clinically significant pharmacological effects. It has been proposed that SST analogue therapy should be temporarily interrupted to avoid possible SSTR blockade, but this needs to be discussed.

Recommended activity

The recommended administered activity is 185–222 MBq (5–6 mCi) in adults and 5 MBq/kg (0.14 mCi/kg) in children.

Administration

Intravenous.

Radiation dosimetry

The effective dose equivalent is about 0.054 mSv/MBq in adults and 0.16 mSv/MBq in children (5 years) [29–31]. There is an additional radiation dose from the CT scan in SPECT/CT protocols (volume CT dose index: 3 to 5 mGy depending on acquisition parameters).

Renal failure

In patients with significant renal failure, high blood pool activity may hamper visualization of uptake foci. After haemodialysis, an interpretable scintigram can be obtained.

Pregnancy

Clinical decision is necessary to consider the benefits against the possible harm of carrying out any procedure in patients known or suspected to be pregnant.

Breast feeding

Breast feeding should be discontinued for 4 days after injection.

Patient preparation

- SST analogues are rarely used in the treatment of PGL/PCC. Short-acting SST analogues may be discontinued for 24 h before $^{111}$In-pentetreotide administration, while long-acting preparations are preferably stopped 5–6 weeks before the study, and patients should be switched to short-acting formulations, if necessary [32, 33].
- Laxatives are advised, especially when the abdomen is the area of interest. The use of laxatives considerably reduces difficulties in interpretation of SPECT/CT scans due to bowel activity.
- To reduce radiation exposure, patients should be well hydrated before and for at least 1 day after injection.

Image acquisition

- Scans are obtained 4 h and 24 h after tracer injection.
- Imaging field

  Images are acquired using two energy peaks at 171 and 245 keV and large field-of-view medium-energy collimators.

  – Anterior and posterior planar views of the H&N (+ right and left lateral views) and thorax, abdomen and pelvis are acquired at 4 h and 24 h (512×512 or 256×256 word matrix and are obtained for 10–15 min per view).
  – SPECT images covering the anatomical regions showing pathological tracer uptake on planar images are clearly helpful when available. The SPECT images are obtained for a 360° orbit (128×128 word matrix, 6° angle steps, 30–45 s per stop). Coregistered CT images (100–130 kV, mAs modulation recommended) from SPECT/CT cameras enable attenuation and facilitate precise localization of any focus of increased tracer. SPECT/CT images are particularly useful over the abdomen. If only one SPECT scan is performed, acquisition at 24 h is preferred because of a higher target-to-background ratio.
- Optional images

  – Acquisitions (SPECT and/or planar views) may be repeated at 48 h for clarification of equivocal abdominal findings.
  – Whole-body imaging may be performed at both imaging time points. For whole-body images, anterior and posterior images are acquired into a 1,024×512

word matrix or a 1,024×256 word matrix for a minimum of 30 min (maximum speed 6 cm/min).

### Reconstruction

SPECT iterative reconstruction or other validated reconstruction protocol that allows accurate visualization of lesions (to be adapted to the clinical setting), and CT-based attenuation correction for SPECT/CT can be performed.. Attenuation correction can be performed on SPECT images alone based on a constant μ before or after processing (e.g. Sorenson, Chang) but it is not usually done. Scatter correction methods using spectral analysis can be used to improve the accuracy of quantification.

### Image analysis

- Visual analysis

  Physiological distribution: Uptake is seen in the spleen, kidney, liver, bowel (visible on 24-h images), and the gallbladder if fasting. Moderate uptake is often seen over the pituitary and the thyroid glands. Normal adrenal glands can also be faintly visible. Other sites with faint uptake are the pituitary and the thyroid glands (increased diffuse uptake in thyroiditis).

  Pathological uptake: As a rule, and especially in the abdomen, accumulation of radioactivity at an abnormal site is considered to represent SSTR binding only if it is present on the scintigrams from the two standard imaging time points.
- Quantification

  The optimal time to quantify tumours is at 24 h after injection or later. Tumour uptake should be scored using visual criteria as follows: 0 no uptake; 1 very low/equivocal uptake; 2 clear, but faint uptake (less than or equal to liver uptake); 3 moderate uptake (higher than liver uptake); 4 intense uptake. This scoring is rather used in selecting candidates for targeted radionuclide therapy.

### Pitfalls

- False-positives

  Renal parapelvic cysts, accessory spleen or abdominal hernia. False-positive results may be related to tracer uptake by other neuroendocrine lesions or other SST2-expressing tumours (thyroid or breast disease are the most frequent causes of false-positive foci) [33]. Since SST2 is overexpressed in activated lymphocytes and macrophages, false-positive images may also be related to granulomatous and inflammatory diseases.
- False-negatives

  Small H&N PGLs, abdominal PGLs.

### Diagnostic accuracy

In parasympathetic H&N PGLs, several studies have demonstrated the superiority of $^{111}$In-pentetreotide scintigraphy compared to $^{131}$I/$^{123}$I-MIBG, with sensitivities of 89–100 % and 18–50 %, respectively [34–39]. However, its sensitivity needs to be revised in patients with hereditary syndromes because some additional lesions can be in the millimetre range and not detectable by conventional scintigraphy [40].

The sensitivity of $^{111}$In-pentetreotide is clearly inferior to that of $^{123}$I-MIBG scintigraphy in abdominal and metastatic PGL, even though it can provide additional information in some patients with rapidly progressing metastatic PGL [20, 41–43]. $^{111}$In-Pentetreotide may also detect other syndromic lesions (e.g. neuroendocrine pancreatic tumour, MTC, or pituitary tumours).

## PET imaging with $^{68}$Ga-conjugated peptides

### Radiopharmaceuticals

SSTRs have been imaged by PET using DOTA-coupled SST agonists (SSTa) labelled with $^{68}$Ga ($^{68}$Ga-conjugated peptides) as tracers. $^{68}$Ge/$^{68}$Ga generators and DOTA peptides do not yet have marketing authorization. $^{68}$Ga-conjugated peptides are available as radiotracers prepared in-house and must fulfil the criteria laid down in the European Pharmacopoeia monographs and/or good radiopharmaceutical practice.$^{68}$Ga is a positron-emitting radioisotope allowing, when labelled with DOTA peptides, PET scanning of SSTR. Due to the short half-life of $^{68}$Ga (68 min), $^{68}$Ga-conjugated peptides are synthesized exclusively on the day of examination.

### Mechanism of cellular uptake

Tracer binding and retention depends on the density of SSTRs on the cell surface and the degree of internalization of the ligand–receptor complex. All radiolabelled DOTA peptides can target SSTR2 effectively, which is the one most overexpressed in PGLs. SST1 is also strongly expressed in some PGLs, while other receptor subtypes are only slightly expressed or not at all. The low expression of SST5 observed in PGLs constitutes a major difference from some endocrine tumours of the gastrointestinal tract.

Currently, three DOTA-coupled peptides (DOTATOC, Tyr3-octreotide; DOTATATE, Tyr3-octreotate; and DOTA-NOC, Nal3-octreotide) have shown excellent affinity for SST2 receptors ($IC_{50}$ 2.5 nM, 0.2 nM, and 1.9 nM, respectively). DOTA-NOC also binds specifically to SST3, SST4 and SST5 receptors. DOTA-TOC also binds to SST5 (although with lower affinity than DOTA-NOC) [44–46].

Pharmacokinetics

After intravenous administration, DOTA peptides concentrate in the kidney (5 %), liver (2 %), spleen (2 %) and pituitary gland (0.02 %). Maximal tumour activity is reached in 60 min. DOTA peptides are mainly excreted by the kidney (40–75 % of the injected dose at 3 and 24 h, respectively, after injection). Less than 2 % of the injected dose is excreted in the faeces up to 48 h.

Synthesis and quality control

Currently, neither $^{68}$Ge/$^{68}$Ga generators nor DOTA-conjugated peptides have marketing authorization and therefore have to be prepared according to the national regulations and good radiopharmaceutical practice and as laid down in the European Pharmacopoeia monographs [GALLIUM (68Ga) EDOTREOTIDE INJECTION]. Radiolabelling of these peptides with $^{68}$Ga is robust (radiochemical purity >95 %), requires between 20 and 30 min, and is entirely automated. Briefly, the labelling procedure is divided into the following steps [47].

- $^{68}$Ga elution: $^{68}$Ge/$^{68}$Ga generators are eluted with hydrochloric acid solution (0.1–1 N).
- DOTA-peptide radiolabelling: radiolabelling is performed using an automated system allowing eluate purification and peptide labelling at an elevated temperature and suitable pH.
- Purification: if necessary, purification can be performed using a chromatographic cartridge. The method used must ensure that the level of $^{68}$Ge is lower than 0.001 % of the total activity and the radiochemical purity of $^{68}$Ga-DOTA-peptide more than 95 %.
- Sterilization: the final solution must be sterilized using sterilizing filtration.
- Quality controls: appearance, pH, bacterial endotoxins, radionucleidic and radiochemical purity must be assessed before injection using validated methods. Sterility testing must be done, but the injection may be released for use before completion of the test.

The amount of DOTA-peptide injected should be less than 50 μg. A blocking effect in the tumour tissue has been reported at higher amounts of DOTA-peptide (250, 500 μg) [48].

Drug interactions and side effects

SST analogues may affect tracer accumulation in organs and in tumour sites.

Recommended activity

The activity administered ranges from 100 to 200 MBq.

Administration

Intravenous.

Radiation dosimetry

The effective dose ranges from 0.0042 to 0.015 μSv/MBq.

Pregnancy

Clinical decision is necessary to consider the benefits against the possible harm of carrying out any procedure in patients known or suspected to be pregnant.

Breast feeding

Breast feeding should be discontinued for 12 h after injection.

Patient preparation

There is no need for fasting before injection. It has been recommended that octreotide therapy be discontinued (1 day for short-lived molecules and 3–4 weeks for long-acting analogues). To date, this issue is still not definitively clarified.

Image acquisition

Scans are usually obtained from 45 to 90 min after tracer injection from the base of the skull to the mid-thighs (or over the whole-body depending on the clinical setting). There is no generally accepted acquisition time in the literature.

Image reconstruction

Data acquired in 3D mode can be reconstructed directly using a 3D reconstruction algorithm or rebinned as 2D data and subsequently reconstructed with a 2D reconstruction algorithm. Iterative reconstruction algorithms are the current standard for clinical routine. CT-based attenuation correction can be performed.

Image analysis

- Visual analysis

  Physiological distribution: the distribution is similar to that of $^{111}$In-DTPA-octreotide. Intense accumulation of radioactivity is seen in the spleen (and accessory spleen if present), kidneys, adrenals and pituitary. Accumulation in the liver is usually less intense than that

noted in the spleen. The thyroid and salivary glands are faintly visible. Additionally, variable tracer uptake is frequently found in the pancreas particularly in the uncinate process [49]. The prostate gland and breast glandular tissue may show diffuse low-grade uptake of $^{68}$Ga-DOTA-conjugated peptides.

- Quantification

  SUV is an easily measured and useful parameter for tumour characterization, if taken in a standardized manner. It is important that the PET/CT system is calibrated for the half-life of $^{68}$Ga.

Pitfalls

- False-positives

  Other diseases characterized by a high SST status, and activated lymphocytes at sites of inflammation may produce false-positive results.

  Pancreatic accumulation (most frequently in the uncinate process) may mimic focal tumour disease in the pancreas.
- False-negatives

  There are insufficient data to draw conclusions regarding sensitivity.

Diagnostic accuracy

The new PET tracers targeting SSTRs are now under evaluation in PGLs and published data are limited to case reports and small series [50–56]. $^{68}$Ga-DOTATOC and $^{68}$Ga-DOTATATE PET/CT has been found to be superior to $^{123}$I-MIBG SPECT in some patients with aggressive PGLs probably because of a certain level of functional dedifferentiation [53].

## $^{18}$F-FDOPA PET

Radiopharmaceutical

*6-[$^{18}$F]Fluoro-L-DOPA*

$^{18}$F-FDOPA is commercially available conditioned in a sterile single-dose or multidose solution for intravenous use. The solution is colourless or pale yellow.

Mechanism of cellular uptake

PCCs/PGLs can take up and decarboxylate amino acids such as dihydroxyphenylalanine (DOPA). This property, common to tumours in the APUD system (Amine Precursor Uptake and Decarboxylation), depends on an enzyme, which catalyses the limiting step in the synthesis of catecholamines: L-aromatic amino acid decarboxylase (AADC). DOPA, the precursor of all endogenous catecholamines, is taken up through a neutral amino acid transporter (LAT1/4F2hc complex). $^{18}$F-FDOPA binds to LAT1 with high affinity and is converted into $^{18}$F-FDA by cytosolic AADC, which enters the catecholamine storage vesicles. It has been shown in different cancer models that LAT1 overexpression is essential for amino acid supply and tumour growth.

Pharmacokinetics

After intravenous administration, $^{18}$F-FDOPA is specifically trapped by tissues expressing LAT1 and follows the metabolic pathways of L-DOPA. Plasmatic $^{18}$F-FDOPA is metabolized by COMT and AAAD. $^{18}$F-FDOPA is quickly converted into $^{18}$F-dopamine in the proximal renal tubule and other target tissues and eliminated in the urine (50 % within 1 h and the rest within 12 h).

PCC/PGLs take up $^{18}$F-FDOPA very quickly. At best, the acquisition for static clinical PET imaging of PCC/PGL with $^{18}$F-FDOPA can start at 20 min after injection for maximum uptake in tumours. After this time, a very slight decrease in the tumour SUV starts, which still amounts to 80 % of the maximum value after 132 min [57]. Some authors report using premedication with carbidopa (an AADC inhibitor) to improve central nervous system bioavailability of the tracer and to decrease physiological uptake by the pancreas [58].

Synthesis and quality control

The synthesis of $^{18}$F-FDOPA requires up to 4 h and suffers from a low labelling yield of between 11 % and 25 % [59, 60]. $^{18}$F-FDOPA can be supplied already labelled in either of two different formulations that conform to the criteria laid down in the European Pharmacopoeia. One is “ready to use”, while the other needs to be extemporaneously neutralized using a bicarbonate buffer kit supplied by the manufacturer. In the second case, the pH needs to be checked and should be kept between 4.0 and 5.0. These two formulations seem to be equivalent, and no additional quality control is needed. Striatum uptake of $^{18}$F-FDOPA suggests integrity of the labelled molecule and can be used as a positive control. $^{18}$F-FDOPA can also be prepared in-house in accordance with the criteria laid down in the European Pharmacopoeia.”

Drug interactions and side effects

Pain during injection has been reported.

Haloperidol and reserpine have been reported to, respectively, increase and decrease striatal $^{18}$F-FDOPA retention [61, 62]. There is no report of drug interaction in PCCs/PGLs.

Recommended activity

4 MBq/kg.

Administration

Intravenous.

Radiation dosimetry

The effective dose equivalent in adults ranges from 0.0199 to 0.0539 mSv/MBq [63–65].

Pregnancy

Clinical decision is necessary to consider the benefits against the possible harm of carrying out any procedure in patients known or suspected to be pregnant.

Breast feeding

Breast feeding should be discontinued for 12 h after treatment.

Patient preparation

Patients should fast for at least 4 h. The administration of 200 mg of carbidopa 1 h prior to $^{18}$F-DOPA injection has been reported to increase tumour uptake [58].

Image acquisition

- Timing of imaging and imaging fields:
  Scans are usually obtained from 30 to 60 min after tracer injection from the base of the skull to the mid-thighs (or over the whole-body depending on the clinical setting).
- Optional images
  - Early images (10 min after tracer injection) centred over the abdomen may be acquired to overcome difficulties in localizing abdominal PGL located near the hepatobiliary system due to physiological tracer elimination.
  - Early images (from 10 to 20 min) centred over the neck may also be acquired in patients with MEN2 with residual hypercalcitoninaemia [66]. MTC lesions often show rapid washout and are better visualized on these early images [67].

Image reconstruction

Data acquired in 3D mode can be reconstructed directly using a 3D reconstruction algorithm or rebinned as 2D data and subsequently reconstructed using a 2D reconstruction algorithm. Iterative reconstruction algorithms represent the current standard for clinical routine. CT-based attenuation correction can also be performed.

Image analysis

- Visual analysis
  Physiological distribution: uptake is seen in the striatum, kidneys, pancreas, liver, gallbladder, biliary tract and duodenum. Adrenal glands can be faintly visible.
  Pathological uptake: any nonphysiological extraadrenal focal uptake or asymmetrical adrenal uptake with a concordant enlarged gland or adrenal uptake more intense than that of the liver with a concordant enlarged gland can be considered pathological.
- Quantification
- SUV is the easiest and most practical parameter to measure.
- The metabolic tumour burden (MTB) is calculated as the product of metabolic tumour volume (MTV) and SUV-mean. MTV can be obtained using the voxels above 40 % (for the $MTV_{40}$) of the maximum count in the tumour volume of interest. The whole-body MTV has been found to correlate with hormonal levels [23].

Pitfalls

- False-positives
  False-positive results may be related to tracer uptake by other neuroendocrine lesions. Rarely, uptake may be due to nonnspecific inflammation (pneumonia, postoperative changes), since high levels of amino acid transport have also been found in macrophages.
- False-negatives
  Small lesions, abdominal SDHx-related PGLs.

Diagnostic accuracy

In a recent metaanalysis of 11 studies (275 patients), the pooled sensitivity and specificity in a per lesion-based analysis of $^{18}$F-FDOPA PET/CT in detecting PCC/PGL were 79 % (95 % CI 76–81 %) and 95 % (95 % CI 84–99 %), respectively [68]. The most significant factors influencing visualization of $^{18}$F-FDOPA-avid foci are tumour location and genetic status. $^{18}$F-FDOPA PET is not a MIBG scan with higher sensitivity, but a new specific radiotracer with its own advantages and limitations [23, 26, 69–74]. Reported sensitivities range from 81 % to 100 %. A special advantage of $^{18}$F-FDOPA PET over $^{123}$I-MIBG and other specific PET tracers stems from its lack of significant uptake in normal adrenal glands [75]. This is particularly helpful in

patients with MEN2. $^{18}$F-FDOPA PET may also detect residual MTC lesions and other syndromic tumours such as pancreatic neuroendocrine tumours that may occur in patients with VHL syndrome (especially after carbidopa premedication).

Several studies have shown that $^{18}$F-FDOPA PET/CT is an excellent first-line imaging tool in H&N PGLs with a sensitivity approaching 100 % [22, 23, 40, 50, 73, 76–78]. It is able to detect tiny jugular lesions that remain occult on conventional morphological imaging. This is due to the high avidity of H&N PGLs for $^{18}$F-FDOPA and the absence of physiological uptake in the adjacent structures (excellent signal-to-noise uptake ratio). The specificity of $^{18}$F-FDOPA PET is similar to that of MIBG scintigraphy. Its sensitivity approaches 100 % in PCCs, but can be lower in extraadrenal retroperitoneal PGLs potentially coexisting with supradiaphragmatic locations in SDHx-related syndromes [22, 23, 40, 68, 73]. In patients with VHL syndrome, $^{18}$F-FDOPA PET may detect pancreatic neuroendocrine tumours [79]. In metastatic disease, $^{18}$F-FDOPA PET most frequently performs better in SDHB-negative patients than in SDHB-positive patients (sensitivity 20 % in carriers of SDHB mutation vs. 93 % in patients without SDHB mutations) [23, 70, 73, 80].

## $^{18}$F-FDG PET

### Radiopharmaceutical

$^{18}$F-FDG is commercially available as a "ready to use" formulation and conditioned in a sterile single-dose or multidose solution for intravenous use.

### Mechanism of cellular uptake

$^{18}$F-FDG is taken up by tumour cells via glucose membrane transporters and phosphorylated by hexokinase into $^{18}$F-FDG-6P. $^{18}$F-FDG-6P does not follow further enzymatic pathways and accumulates in proportion to the glycolytic cellular rate. It is remarkable that many genes (SDHx, VHL) involved in tumorigenesis regulate energy metabolism and cellular responses to hypoxic stress. Inactivation of VHL and SDHx genes upregulates HIF-$\alpha$ (hypoxia-inducible factor) and specific HIF downstream targets including GLUT transporters [81–85] resulting in increased $^{18}$F-FDG uptake in PCC/PGL [86].

### Pharmacokinetics

After intravenous administration, $^{18}$F-FDG is rapidly cleared from the blood, and concentrates in the heart (3 %), lung (1–2 %), spleen (0.3 %) and liver (0.3 %). There is also high uptake in the brain. The majority of the $^{18}$F-FDG is excreted unaltered via the kidneys (20 % of the injected dose is recovered in the urine within 2 h).

### Synthesis and quality control

$^{18}$F-FDG is commercially available or is prepared in-house in a "ready to use" formulation and conforms to the criteria laid down in the European Pharmacopeia.

### Drug interactions and side effects

Blood glucose levels are measured before administering FDG, and thereby detect any drug interaction with glucose metabolism should be detected. Chemotherapy may change FDG tumour uptake by altering cellular metabolism. The timing of restaging with PET depends on the therapy (from 2 to 5 weeks after the end of chemotherapy in patients with metastatic tumours).

### Recommended activity

2–5 MBq/kg.

### Administration

Intravenous.

### Radiation dosimetry

The effective dose equivalent is $2\times10^{-2}$ mSv/MBq.

### Pregnancy

Clinical decision is necessary to consider the benefits against the possible harm of carrying out any procedure in patients known or suspected to be pregnant.

### Breast feeding

Breast feeding should be discontinued for 12 h after imaging.

### Patient preparation

Patients must fast for at least 6 h prior to FDG injection. Patients with PCC and secondary diabetes (about 35 % of patients) require specific instructions for glucose control. During FDG injection and the subsequent uptake phase, patients should remain seated or recumbent, and kept warm, in a darkened and quiet room.

Image acquisition

- Timing of imaging
  Scans are usually obtained at 60 min (45 to 90 min) after injection.
- Imaging field
  From the base of the skull to the mid-thighs (or whole-body imaging, depending on the clinical setting).

Image reconstruction

Data acquired in 3D mode can be reconstructed directly using a 3D reconstruction algorithm or rebinned as 2D data and subsequently reconstructed using a 2D reconstruction algorithm. Iterative reconstruction algorithms are the current standard for clinical routine. CT-based attenuation correction can also be performed.

Image analysis

- Visual analysis
  Physiological distribution: uptake can be seen in the brain cortex, salivary glands, lymphatic tissue of the Waldeyer's ring, muscles, brown fat, myocardium, mediastinum, liver, kidneys and bladder, gastrointestinal tract, testes, uterus and ovaries (before menopause). Physiological $^{18}$F-FDG uptake in brown adipose tissue occurs predominantly in younger patients. In patients with NE-secreting PCC/PGL, there is an increase in uptake in brown adipose tissue due to stimulation of brown adipocytes by NE. The level of physiological $^{18}$F-FDG uptake in normal adrenal glands is low even after contralateral adrenalectomy for PCC but contrasts with the enhanced uptake observed after adrenalectomy for cancer of the adrenal cortex [75, 87].
  Pathological uptake: any nonphysiological extraadrenal focal uptake or adrenal uptake more intense than that of the liver with a concordant enlarged gland can be considered pathological.
- Quantification
  SUV is the easiest parameter to measure for tumour characterization. SUV provides an estimate of normalized tumour uptake, with no simple relationship with the glucose metabolic rate. Additional methods may be used for evaluation of metabolic response to treatment in malignant forms. However, such methods are currently under development and need to be refined and standardized. In any case, images have to be acquired before and after treatment in quasi-identical conditions to observe changes related to the tumours only. FDG uptake is influenced by many factors, of which the most are biological (e.g. histology, genetic status) and physical (partial volume effect, motion artefacts) [88].

Pitfalls

- False-positives
  Several potential diagnoses should be considered in patients with a highly avid adrenal mass (an adrenal to liver SUVmax ratio of >2): adrenocortical carcinoma, primary lymphoma, metastasis, myelolipoma (uptake by the myeloid tissue component of the mass) and oncocytoma. When a mass is moderately avid for $^{18}$F-FDG, other aetiologies should be considered: adrenal cortex adenoma, ganglioneuroma, metastasis (small lesions or from cancer with lower malignant potential, sarcoma), haematoma and adrenocortical hyperplasia. Extraadrenal uptake may be due to inflammatory and neoplastic processes.
- False-negatives
  Sporadic PCCs and retroperitoneal extraadrenal PGLs, MEN2-related PCC, H&N PGL.

Diagnostic accuracy

The most significant factors influencing visualization of $^{18}$F-FDG-avid PGL foci are tumour location, genetic status and degree of tissue differentiation. $^{18}$F-FDG PET positivity is almost a constant feature of PCCs. This finding contrasts with the observation that other endocrine tumours usually exhibit high $^{18}$F-FDG uptake in the later stages of the disease. Some features are suggestive of PCC (e.g. well-limited tumour without vena cava involvement, and decreased uptake in the central area indicating parenchymal degeneration, and calcifications on unenhanced CT images). Uptake may be widely variable between PCCs. Sensitivity and negative predictive value are very high (80–100 %), but the positive predictive value is lower due to lack of specificity of $^{18}$F-FDG. The sensitivity of $^{18}$F-FDG PET is also mainly influenced by the genetic status of the patient [87, 89]. In patients with a MEN2-related PCC, $^{18}$F-FDG PET is 40 % sensitive. $^{18}$F-FDG PET may also detect other syndromic lesions (e.g. gastrointestinal stromal tumour, renal cell carcinoma, pancreatic tumour, MTC, or pituitary tumour) [79]. $^{18}$F-FDG PET is also more frequently helpful in metastatic disease with SDHB mutations and might be suboptimal in other patients (sensitivity per lesion 83 % in SDHB-positive vs. 62 % in SDHB-negative patients).

## Other PET tracers

$^{99m}$Tc-Hydrazinonicotinamide-Tyr(3)-octreotide ($^{99m}$Tc-TOC) is increasingly gaining acceptance as a new

radiopharmaceutical for diagnosis of SSTR-expressing tumours [90, 91]. $^{18}$F-FDA (fluorodopamine) PET has been developed at the National Institutes of Health in Bethesda, MD, and is currently used as an experimental tracer at the NIH only. $^{18}$F-FDA is captured by tumour cells via the NET and stored in intracellular vesicles. $^{18}$F-FDA PET seems to be a very promising tool in the management of PGLs associated with the sympathetic system [20, 21, 92, 93]. $^{11}$C-Hydroxyephedrine ($^{11}$C-HED) has also been evaluated, but its synthesis is complex and the short half-life of $^{11}$C is a major drawback to its routine clinical use [94–98]. MIBG analogues for PET imaging have been used in a few studies, but to our knowledge, no clinical studies have yet been reported [99–101]. The influence of some new drugs (histone deacetylase inhibitors) on tracer uptake is also under investigation [102].

## Recommendations for clinical practice

Successful PCC/PGL management requires an multidisciplinary team approach. Precise identification of the clinical context and genetic status of patients enables personalized use of functional imaging modalities [1, 87, 103, 104] (Fig. 1). It is expected that the early detection of PCC/PGL with modern PET imaging will very soon lead to the best staging of these tumours, thus minimizing complications related to the mass effect and hormone excess, facilitating the most appropriate curative treatment options and reducing the risk of metastatic spread.

### Apparently sporadic nonmetastatic PCCs

$^{123}$I-MIBG is as sensitive as PET imaging ($^{18}$F-FDOPA PET, $^{18}$F-FDA PET, $^{18}$F-FDG), and definitely superior to $^{111}$In-pentetreotide SPECT(/CT) in localizing nonmetastatic sporadic PCC. $^{123}$I-MIBG scintigraphy appears sufficient to confirm the diagnosis of PCC even in rare cases of non-hypersecreting PCC. With its ability for whole-body screening, it can rule out extraadrenal disease and act as a guide for additional CT and MRI investigations. There is no clear advantage of using PET tracers over $^{123}$I-MIBG scintigraphy in these patients. Their use should be reserved for MIBG-negative cases, multifocal tumours on $^{123}$I-MIBG scintigraphy and/or patients taking drugs that significantly interfere with the accuracy of $^{123}$I-MIBG scintigraphy.

### H&N PGLs

$^{18}$F-FDOPA PET appears to be the most sensitive imaging tool for these tumours in general with a sensitivity approaching 100 %. In the absence of $^{18}$F-FDOPA, SSTR scintigraphy with $^{111}$In-pentetreotide SPECT(/CT) acquisition may be used as the first-line evaluation. PET imaging with $^{68}$Ga-conjugated peptide SST analogues seems to be highly sensitive and deserves to be compared with $^{18}$F-FDOPA in clinical trials. $^{123}$I-MIBG scintigraphy and $^{18}$F-FDA PET are not sufficiently sensitive. $^{18}$F-FDG PET has high sensitivity in the setting of SDHx-related H&N PGLs and may help detect additional thoracic/abdominal tumours.

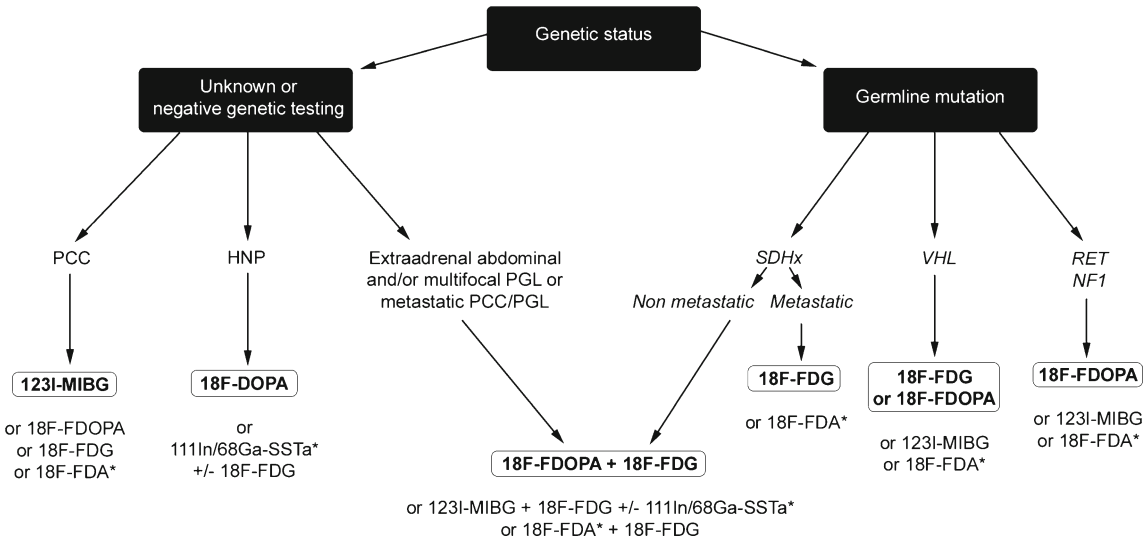


**Fig. 1** Clinical algorithm for imaging investigations in PCC/PGL. Based on the above considerations, the following algorithm can be proposed based on the clinical situation. This algorithm should be adapted to the practical situation in each institution, and should evolve with time. *In bold* First-line imaging procedures according to accessibility of tracers and clinical approvals in European countries. $^{18}$F-FDA and $^{68}$Ga-DOTA-SSTa (*asterisks*) are experimental tracers that should be used in the setting of clinical trials. $^{18}$F-FDA PET is currently used at the NIH only. $^{68}$Ga-DOTA-SSTa is now accessible in many clinical and research centres in Europe

Retroperitoneal extraadrenal nonmetastatic PGLs

In patients with a retroperitoneal extraadrenal nonrenal mass, imaging should differentiate a PGL from a neurogenic tumour, lymph node diseases, or a mesenchymal tumour. Therefore, the specificity of functional imaging provides an important contribution. Once the diagnosis of PGL has been established, the multiplicity of extraadrenal localizations should be considered.

$^{18}$F-FDOPA PET has higher sensitivity than $^{123}$I-MIBG scintigraphy, and is more specific than $^{18}$F-FDG PET. Therefore, at present, $^{18}$F-FDOPA PET is probably the preferred imaging modality when PGL is suspected. $^{18}$F-FDG PET is especially sensitive in the setting of SDHx- and VHL-related sympathetic PGLs. $^{18}$F-FDA PET has the highest sensitivity and specificity across genetically different PGLs, but suffers from its limited availability.

Metastatic PCC/PGL

Several studies have demonstrated the limitations of using $^{123}$I-MIBG scintigraphy alone in the staging and restaging of hereditary and metastatic PCCs/PGLs. The use of $^{123}$I-MIBG may lead to significant underestimation of metastatic disease with potentially inappropriate management. $^{18}$F-FDG PET is the imaging modality of choice for SDHB-related metastatic PCCs/PGLs. $^{18}$F-FDOPA PET/CT may be the imaging modality of choice in the absence of SDHB mutations, or when genetic status is unknown. Once it becomes more widely available, $^{18}$F-FDA PET might be used as a first-line diagnostic imaging modality in patients with metastatic PCCs/PGLs, whatever their genetic status. The main purpose of $^{123}$I-MIBG or $^{111}$In-DTPA-octreotide scintigraphy in a patient with metastases is to determine if internal targeted radiotherapy is an appropriate treatment choice.

MEN2-related PCC

Limited data are available in the literature with respect to imaging studies in patients with MEN2. Many of these patients do not need any specific functional imaging if a tumour is confined to the adrenal gland with concomitant and characteristic elevation of plasma or urine metanephrine levels. $^{123}$I-MIBG scintigraphy can be used in the detection of these tumours, but sensitivity and specificity are suboptimal. The absence of high $^{18}$F-FDOPA uptake by healthy adrenal glands is an interesting feature in the diagnosis, staging and restaging of MEN2-related PCC. $^{18}$F-FDG PET is not sufficiently sensitive in this clinical setting.

**Conflicts of interest** None.

## References


1. Taieb D, Neumann H, Rubello D, Al-Nahhas A, Guillet B, Hindie E. Modern nuclear imaging for paragangliomas: beyond SPECT. J Nucl Med. 2012;53:264–74.
2. Karasek D, Shah U, Frysak Z, Stratakis C, Pacak K. An update on the genetics of pheochromocytoma. J Hum Hypertens. 2012
3. Rutgers M, Tytgat GA, Verwijs-Janssen M, Buitenhuis C, Voute PA, Smets LA. Uptake of the neuron-blocking agent meta-iodobenzylguanidine and serotonin by human platelets and neuro-adrenergic tumour cells. Int J Cancer. 1993;54:290–5.
4. Jaques Jr S, Tobes MC, Sisson JC. Sodium dependency of uptake of norepinephrine and m-iodobenzylguanidine into cultured human pheochromocytoma cells: evidence for uptake-one. Cancer Res. 1987;47:3920–8.
5. Bomanji J, Levison DA, Flatman WD, Horne T, Bouloux PM, Ross G, et al. Uptake of iodine-123 MIBG by pheochromocytomas, paragangliomas, and neuroblastomas: a histopathological comparison. J Nucl Med. 1987;28:973–8.
6. Sinclair AJ, Bomanji J, Harris P, Ross G, Besser GM, Britton KE. Pre- and post-treatment distribution pattern of 123I-MIBG in patients with phaeochromocytomas and paragangliomas. Nucl Med Commun. 1989;10:567–76.
7. Solanki KK, Bomanji J, Moyes J, Mather SJ, Trainer PJ, Britton KE. A pharmacological guide to medicines which interfere with the biodistribution of radiolabelled meta-iodobenzylguanidine (MIBG). Nucl Med Commun. 1992;13:513–21.
8. Bombardieri E, Aktolun C, Baum RP, Bishof-Delaloye A, Buscombe J, Chatal JF, et al. 131I/123I-metaiodobenzylguanidine (MIBG) scintigraphy: procedure guidelines for tumour imaging. Eur J Nucl Med Mol Imaging. 2003;30:BP132–9.
9. Bombardieri E, Giammarile F, Aktolun C, Baum RP, Bischof Delaloye A, Maffioli L, et al. 131I/123I-metaiodobenzylguanidine (mIBG) scintigraphy: procedure guidelines for tumour imaging. Eur J Nucl Med Mol Imaging. 2010;37:2436–46.
10. Khafagi FA, Shapiro B, Fig LM, Mallette S, Sisson JC. Labetalol reduces iodine-131 MIBG uptake by pheochromocytoma and normal tissues. J Nucl Med. 1989;30:481–9.
11. Apeldoorn L, Voerman HJ, Hoefnagel CA. Interference of MIBG uptake by medication: a case report. Neth J Med. 1995;46:239–43.
12. Estorch M, Carrio I, Mena E, Flotats A, Camacho V, Fuertes J, et al. Challenging the neuronal MIBG uptake by pharmacological intervention: effect of a single dose of oral amitriptyline on regional cardiac MIBG uptake. Eur J Nucl Med Mol Imaging. 2004;31:1575–80.
13. Zaplatnikov K, Menzel C, Dobert N, Hamscho N, Kranert WT, Gotthard M, et al. Case report: drug interference with MIBG uptake in a patient with metastatic paraganglioma. Br J Radiol. 2004;77:525–7.
14. Blake GM, Lewington VJ, Fleming JS, Zivanovic MA, Ackery DM. Modification by nifedipine of 131I-meta-iodobenzylguanidine kinetics in malignant phaeochromocytoma. Eur J Nucl Med. 1988;14:345–8.
15. Taniguchi K, Ishizu K, Torizuka T, Hasegawa S, Okawada T, Ozawa T, et al. Metastases of predominantly dopamine-secreting phaeochromocytoma that did not accumulate meta-iodobenzylguanidine: imaging with whole body positron emission tomography using 18F-labelled deoxyglucose. Eur J Surg. 2001;167:866–70.
16. Van Der Horst-Schrivers AN, Osinga TE, Kema IP, Van Der Laan BF, Dullaart RP. Dopamine excess in patients with head and neck paragangliomas. Anticancer Res. 2010;30:5153–8.
17. van Gelder T, Verhoeven GT, de Jong P, Oei HY, Krenning EP, Vuzevski VD, et al. Dopamine-producing paraganglioma not visualized by iodine-123-MIBG scintigraphy. J Nucl Med. 1995;36:620–2.

18. Hall FT, Perez-Ordonez B, Mackenzie RG, Gilbert RW. Does catecholamine secretion from head and neck paragangliomas respond to radiotherapy? Case report and literature review. Skull Base. 2003;13:229–34.
19. Tobes MC, Fig LM, Carey J, Geatti O, Sisson JC, Shapiro B. Alterations of iodine-131 MIBG biodistribution in an anephric patient: comparison to normal and impaired renal function. J Nucl Med. 1989;30:1476–82.
20. Ilias I, Chen CC, Carrasquillo JA, Whatley M, Ling A, Lazurova I, et al. Comparison of 6-18F-fluorodopamine PET with 123I-metaiodobenzylguanidine and 111In-pentetreotide scintigraphy in localization of nonmetastatic and metastatic pheochromocytoma. J Nucl Med. 2008;49:1613–9.
21. Timmers HJ, Eisenhofer G, Carrasquillo JA, Chen CC, Whatley M, Ling A, et al. Use of 6-[18F]-fluorodopamine positron emission tomography (PET) as first-line investigation for the diagnosis and localization of non-metastatic and metastatic phaeochromocytoma (PHEO). Clin Endocrinol (Oxf). 2009;71:11–7.
22. Timmers HJ, Chen CC, Carrasquillo JA, Whatley M, Ling A, Havekes B, et al. Comparison of 18F-fluoro-L-DOPA, 18F-fluoro-deoxyglucose, and 18F-fluorodopamine PET and 123I-MIBG scintigraphy in the localization of pheochromocytoma and paraganglioma. J Clin Endocrinol Metab. 2009;94:4757–67.
23. Fiebrich HB, Brouwers AH, Kerstens MN, Pijl ME, Kema IP, de Jong JR, et al. 6-[F-18]Fluoro-L-dihydroxyphenylalanine positron emission tomography is superior to conventional imaging with (123)I-metaiodobenzylguanidine scintigraphy, computer tomography, and magnetic resonance imaging in localizing tumors causing catecholamine excess. J Clin Endocrinol Metab. 2009;94:3922–30.
24. Fonte JS, Robles JF, Chen CC, Reynolds J, Whatley M, Ling A, et al. False-negative 123I-MIBG SPECT is most commonly found in SDHB-related pheochromocytoma or paraganglioma with high frequency to develop metastatic disease. Endocr Relat Cancer. 2012;19:83–93.
25. Kaji P, Carrasquillo JA, Linehan WM, Chen CC, Eisenhofer G, Pinto PA, et al. The role of 6-[18F]fluorodopamine positron emission tomography in the localization of adrenal pheochromocytoma associated with von Hippel-Lindau syndrome. Eur J Endocrinol. 2007;156:483–7.
26. Hoegerle S, Nitzsche E, Altehoefer C, Ghanem N, Manz T, Brink I, et al. Pheochromocytomas: detection with 18F DOPA whole body PET – initial results. Radiology. 2002;222:507–12.
27. Krenning EP, Bakker WH, Kooij PP, Breeman WA, Oei HY, de Jong M, et al. Somatostatin receptor scintigraphy with indium-111-DTPA-D-Phe-1-octreotide in man: metabolism, dosimetry and comparison with iodine-123-Tyr-3-octreotide. J Nucl Med. 1992;33:652–8.
28. Bombardieri E, Ambrosini V, Aktolun C, Baum RP, Bishof-Delaloye A, Del Vecchio S, et al. 111In-pentetreotide scintigraphy: procedure guidelines for tumour imaging. Eur J Nucl Med Mol Imaging. 2010;37:1441–8.
29. Kwekkeboom DJ, Kooij PP, Bakker WH, Macke HR, Krenning EP. Comparison of 111In-DOTA-Tyr3-octreotide and 111In-DTPA-octreotide in the same patients: biodistribution, kinetics, organ and tumor uptake. J Nucl Med. 1999;40:762–7.
30. Stabin MG, Kooij PP, Bakker WH, Inoue T, Endo K, Coveney J, et al. Radiation dosimetry for indium-111-pentetreotide. J Nucl Med. 1997;38:1919–22.
31. Bombardieri E, Aktolun C, Baum RP, Bishof-Delaloye A, Buscombe J, Chatal JF, et al. 111In-pentetreotide scintigraphy: procedure guidelines for tumour imaging. Eur J Nucl Med Mol Imaging. 2003;30:BP140–7.
32. Balon HR. Updated practice guideline for somatostatin receptor scintigraphy. J Nucl Med. 2011;52:1838.
33. Balon HR, Brown TL, Goldsmith SJ, Silberstein EB, Krenning EP, Lang O, et al. The SNM practice guideline for somatostatin receptor scintigraphy 2.0. J Nucl Med Technol. 2011;39:317–24.
34. Bustillo A, Telischi F, Weed D, Civantos F, Angeli S, Serafini A, et al. Octreotide scintigraphy in the head and neck. Laryngoscope. 2004;114:434–40.
35. Duet M, Sauvaget E, Petelle B, Rizzo N, Guichard JP, Wassef M, et al. Clinical impact of somatostatin receptor scintigraphy in the management of paragangliomas of the head and neck. J Nucl Med. 2003;44:1767–74.
36. Koopmans KP, Jager PL, Kema IP, Kerstens MN, Albers F, Dullaart RP. 111In-octreotide is superior to 123I-metaiodobenzylguanidine for scintigraphic detection of head and neck paragangliomas. J Nucl Med. 2008;49:1232–7.
37. Muros MA, Llamas-Elvira JM, Rodriguez A, Ramirez A, Gomez M, Arraez MA, et al. 111In-pentetreotide scintigraphy is superior to 123I-MIBG scintigraphy in the diagnosis and location of chemodectoma. Nucl Med Commun. 1998;19:735–42.
38. Schmidt M, Fischer E, Dietlein M, Michel O, Weber K, Moka D, et al. Clinical value of somatostatin receptor imaging in patients with suspected head and neck paragangliomas. Eur J Nucl Med Mol Imaging. 2002;29:1571–80.
39. Telischi FF, Bustillo A, Whiteman ML, Serafini AN, Reisberg MJ, Gomez-Marin O, et al. Octreotide scintigraphy for the detection of paragangliomas. Otolaryngol Head Neck Surg. 2000;122:358–62.
40. Charrier N, Deveze A, Fakhry N, Sebag F, Morange I, Gaborit B, et al. Comparison of [111In]pentetreotide-SPECT and [18F] FDOPA-PET in the localization of extra-adrenal paragangliomas: the case for a patient-tailored use of nuclear imaging modalities. Clin Endocrinol (Oxf). 2011;74:21–9.
41. Kaltsas GA, Mukherjee JJ, Grossman AB. The value of radiolabelled MIBG and octreotide in the diagnosis and management of neuroendocrine tumours. Ann Oncol. 2001;12 Suppl 2:S47–50.
42. van der Harst E, de Herder WW, Bruining HA, Bonjer HJ, de Krijger RR, Lamberts SW, et al. [(123)I]metaiodobenzylguanidine and [(111)In]octreotide uptake in benign and malignant pheochromocytomas. J Clin Endocrinol Metab. 2001;86:685–93.
43. Tenenbaum F, Lumbroso J, Schlumberger M, Mure A, Plouin PF, Caillou B, et al. Comparison of radiolabeled octreotide and metaiodobenzylguanidine (MIBG) scintigraphy in malignant pheochromocytoma. J Nucl Med. 1995;36:1–6.
44. Wild D, Macke HR, Waser B, Reubi JC, Ginj M, Rasch H, et al. 68Ga-DOTANOC: a first compound for PET imaging with high affinity for somatostatin receptor subtypes 2 and 5. Eur J Nucl Med Mol Imaging. 2005;32:724.
45. Wild D, Schmitt JS, Ginj M, Macke HR, Bernard BF, Krenning E, et al. DOTA-NOC, a high-affinity ligand of somatostatin receptor subtypes 2, 3 and 5 for labelling with various radiometals. Eur J Nucl Med Mol Imaging. 2003;30:1338–47.
46. Reubi JC, Schar JC, Waser B, Wenger S, Heppeler A, Schmitt JS, et al. Affinity profiles for human somatostatin receptor subtypes SST1-SST5 of somatostatin radiotracers selected for scintigraphic and radiotherapeutic use. Eur J Nucl Med. 2000;27:273–82.
47. Virgolini I, Ambrosini V, Bomanji JB, Baum RP, Fanti S, Gabriel M, et al. Procedure guidelines for PET/CT tumour imaging with 68Ga-DOTA-conjugated peptides: 68Ga-DOTA-TOC, 68Ga-DOTA-NOC, 68Ga-DOTA-TATE. Eur J Nucl Med Mol Imaging. 2010;37:2004–10.
48. Velikyan I, Sundin A, Eriksson B, Lundqvist H, Sorensen J, Bergstrom M, et al. In vivo binding of [68Ga]-DOTATOC to somatostatin receptors in neuroendocrine tumours – impact of peptide mass. Nucl Med Biol. 2010;37:265–75.
49. Castellucci P, Pou Ucha J, Fuccio C, Rubello D, Ambrosini V, Montini GC, et al. Incidence of increased 68Ga-DOTANOC uptake in the pancreatic head in a large series of extrapancreatic NET

patients studied with sequential PET/CT. J Nucl Med. 2011;52:886–90.
50. Fanti S, Ambrosini V, Tomassetti P, Castellucci P, Montini G, Allegri V, et al. Evaluation of unusual neuroendocrine tumours by means of 68Ga-DOTA-NOC PET. Biomed Pharmacother. 2008;62:667–71.
51. Naji M, Zhao C, Welsh SJ, Meades R, Win Z, Ferrarese A, et al. 68Ga-DOTA-TATE PET vs. 123I-MIBG in identifying malignant neural crest tumours. Mol Imaging Biol. 2011;13:769–75.
52. Win Z, Rahman L, Murrell J, Todd J, Al-Nahhas A. The possible role of 68Ga-DOTATATE PET in malignant abdominal paraganglioma. Eur J Nucl Med Mol Imaging. 2006;33:506.
53. Naji M, Al-Nahhas A. (68)Ga-labelled peptides in the management of neuroectodermal tumours. Eur J Nucl Med Mol Imaging. 2012;39 Suppl 1:61–7.
54. Win Z, Al-Nahhas A, Towey D, Todd JF, Rubello D, Lewington V, et al. 68Ga-DOTATATE PET in neuroectodermal tumours: first experience. Nucl Med Commun. 2007;28:359–63.
55. Grassi I, Nanni C, Vicennati V, Castellucci P, Allegri V, Montini GC, et al. I-123 MIBG scintigraphy and 68Ga-DOTANOC PET/CT negative but F-18 DOPA PET/CT positive pheochromocytoma: a case report. Clin Nucl Med. 2011;36:124–6.
56. Naswa N, Sharma P, Nazar AH, Agarwal KK, Kumar R, Ammini AC, et al. Prospective evaluation of 68Ga-DOTA-NOC PET-CT in phaeochromocytoma and paraganglioma: preliminary results from a single centre study. Eur Radiol. 2012;22:710–9.
57. Hentschel M, Rottenburger C, Boedeker CC, Neumann HP, Brink I. Is there an optimal scan time for 6-[F-18]fluoro-L-DOPA PET in pheochromocytomas and paragangliomas? Clin Nucl Med. 2012;37:e24–9.
58. Timmers HJ, Hadi M, Carrasquillo JA, Chen CC, Martiniova L, Whatley M, et al. The effects of carbidopa on uptake of 6-18F-Fluoro-L-DOPA in PET of pheochromocytoma and extraadrenal abdominal paraganglioma. J Nucl Med. 2007;48:1599–606.
59. Luxen A, Perlmutter M, Bida GT, Van Moffaert G, Cook JS, Satyamurthy N, et al. Remote, semiautomated production of 6-[18F]fluoro-L-dopa for human studies with PET. Int J Rad Appl Instrum A. 1990;41:275–81.
60. Namavari M, Bishop A, Satyamurthy N, Bida G, Barrio JR. Regioselective radiofluorodestannylation with [18F]F2 and [18F]CH3COOF: a high yield synthesis of 6-[18F]Fluoro-L-dopa. Int J Rad Appl Instrum A. 1992;43:989–96.
61. Vernaleken I, Kumakura Y, Cumming P, Buchholz HG, Siessmeier T, Stoeter P, et al. Modulation of [18F]fluorodopa (FDOPA) kinetics in the brain of healthy volunteers after acute haloperidol challenge. Neuroimage. 2006;30:1332–9.
62. Garnett S, Firnau G, Nahmias C, Chirakal R. Striatal dopamine metabolism in living monkeys examined by positron emission tomography. Brain Res. 1983;280:169–71.
63. Brown WD, Oakes TR, DeJesus OT, Taylor MD, Roberts AD, Nickles RJ, et al. Fluorine-18-fluoro-L-DOPA dosimetry with carbidopa pretreatment. J Nucl Med. 1998;39:1884–91.
64. Harvey J, Firnau G, Garnett ES. Estimation of the radiation dose in man due to 6-[18F]fluoro-L-dopa. J Nucl Med. 1985;26:931–5.
65. Dhawan V, Belakhlef A, Robeson W, Ishikawa T, Margouleff C, Takikawa S, et al. Bladder wall radiation dose in humans from fluorine-18-FDOPA. J Nucl Med. 1996;37:1850–2.
66. Beheshti M, Pocher S, Vali R, Waldenberger P, Broinger G, Nader M, et al. The value of 18F-DOPA PET-CT in patients with medullary thyroid carcinoma: comparison with 18F-FDG PET-CT. Eur Radiol. 2009;19:1425–34.
67. Soussan M, Nataf V, Kerrou K, Grahek D, Pascal O, Talbot JN, et al. Added value of early 18F-FDOPA PET/CT acquisition time in medullary thyroid cancer. Nucl Med Commun. 2012;33:775–9.
68. Treglia G, Cocciolillo F, de Waure C, Di Nardo F, Gualano MR, Castaldi P, et al. Diagnostic performance of 18F-dihydroxyphenylalanine positron emission tomography in patients with paraganglioma: a meta-analysis. Eur J Nucl Med Mol Imaging. 2012;39:1144–53.
69. Mackenzie IS, Gurnell M, Balan KK, Simpson H, Chatterjee K, Brown MJ. The use of 18-fluoro-dihydroxyphenylalanine and 18-fluorodeoxyglucose positron emission tomography scanning in the assessment of metaiodobenzylguanidine-negative phaeochromocytoma. Eur J Endocrinol. 2007;157:533–7.
70. Imani F, Agopian VG, Auerbach MS, Walter MA, Imani F, Benz MR, et al. 18F-FDOPA PET and PET/CT accurately localize pheochromocytomas. J Nucl Med. 2009;50:513–9.
71. Kauhanen S, Seppanen M, Ovaska J, Minn H, Bergman J, Korsoff P, et al. The clinical value of [18F]fluoro-dihydroxyphenylalanine positron emission tomography in primary diagnosis, staging, and restaging of neuroendocrine tumors. Endocr Relat Cancer. 2009;16:255–65.
72. Luster M, Karges W, Zeich K, Pauls S, Verburg FA, Dralle H, et al. Clinical value of 18F-fluorodihydroxyphenylalanine positron emission tomography/computed tomography (18F-DOPA PET/CT) for detecting pheochromocytoma. Eur J Nucl Med Mol Imaging. 2010;37:484–93.
73. Fottner C, Helisch A, Anlauf M, Rossmann H, Musholt TJ, Kreft A, et al. 6-18F-fluoro-L-dihydroxyphenylalanine positron emission tomography is superior to 123I-metaiodobenzyl-guanidine scintigraphy in the detection of extraadrenal and hereditary pheochromocytomas and paragangliomas: correlation with vesicular monoamine transporter expression. J Clin Endocrinol Metab. 2010;95:2800–10.
74. Rufini V, Treglia G, Castaldi P, Perotti G, Calcagni ML, Corsello SM, et al. Comparison of 123I-MIBG SPECT-CT and 18F-DOPA PET-CT in the evaluation of patients with known or suspected recurrent paraganglioma. Nucl Med Commun. 2011;32:575–82.
75. Leboulleux S, Deandreis D, Escourrou C, Al Ghuzlan A, Bidault F, Auperin A, et al. Fluorodesoxyglucose uptake in the remaining adrenal glands during the follow-up of patients with adrenocortical carcinoma: do not consider it as malignancy. Eur J Endocrinol. 2011;164:89–94.
76. Hoegerle S, Ghanem N, Altehoefer C, Schipper J, Brink I, Moser E, et al. 18F-DOPA positron emission tomography for the detection of glomus tumours. Eur J Nucl Med Mol Imaging. 2003;30:689–94.
77. King KS, Chen CC, Alexopoulos DK, Whatley MA, Reynolds JC, Patronas N, et al. Functional imaging of SDHx-related head and neck paragangliomas: comparison of 18F-fluorodihydroxyphenylalanine, 18F-fluorodopamine, 18F-fluoro-2-deoxy-D-glucose PET, 123I-metaiodobenzylguanidine scintigraphy, and 111In-pentetreotide scintigraphy. J Clin Endocrinol Metab. 2011;96:2779–85.
78. King KS, Whatley MA, Alexopoulos DK, Reynolds JC, Chen CC, Mattox DE, et al. The use of functional imaging in a patient with head and neck paragangliomas. J Clin Endocrinol Metab. 2010;95:481–2.
79. Weisbrod AB, Kitano M, Gesuwan K, Millo C, Herscovitch P, Nilubol N, et al. Clinical utility of functional imaging with 18F-FDOPA in Von Hippel-Lindau syndrome. J Clin Endocrinol Metab. 2012;97:E613–7.
80. Taieb D, Tessonnier L, Sebag F, Niccoli-Sire P, Morange I, Colavolpe C, et al. The role of 18F-FDOPA and 18F-FDG-PET in the management of malignant and multifocal phaeochromocytomas. Clin Endocrinol (Oxf). 2008;69:580–6.
81. Favier J, Briere JJ, Burnichon N, Riviere J, Vescovo L, Benit P, et al. The Warburg effect is genetically determined in inherited pheochromocytomas. PLoS One. 2009;4:e7094.
82. Lopez-Jimenez E, Gomez-Lopez G, Leandro-Garcia LJ, Munoz I, Schiavi F, Montero-Conde C, et al. Research resource: transcriptional profiling reveals different pseudohypoxic signatures in SDHB and VHL-related pheochromocytomas. Mol Endocrinol. 2010;24:2382–91.
83. Burnichon N, Vescovo L, Amar L, Libe R, de Reynies A, Venisse A, et al. Integrative genomic analysis reveals somatic mutations

in pheochromocytoma and paraganglioma. Hum Mol Genet. 2011;20:3974–85.
84. Pollard PJ, El-Bahrawy M, Poulsom R, Elia G, Killick P, Kelly G, et al. Expression of HIF-1alpha, HIF-2alpha (EPAS1), and their target genes in paraganglioma and pheochromocytoma with VHL and SDH mutations. J Clin Endocrinol Metab. 2006;91:4593–8.
85. Span PN, Rao JU, Oude Ophuis SB, Lenders JW, Sweep FC, Wesseling P, et al. Overexpression of the natural antisense hypoxia-inducible factor-1alpha transcript is associated with malignant pheochromocytoma/paraganglioma. Endocr Relat Cancer. 2011;18:323–31.
86. Taieb D, Sebag F, Barlier A, Tessonnier L, Palazzo FF, Morange I, et al. 18F-FDG avidity of pheochromocytomas and paragangliomas: a new molecular imaging signature? J Nucl Med. 2009;50:711–7.
87. Timmers HJ, Chen CC, Carrasquillo JA, Whatley M, Ling A, Eisenhofer G, et al. Staging and functional characterization of pheochromocytoma and paraganglioma by 18F-fluorodeoxyglucose (18F-FDG) positron emission tomography. J Natl Cancer Inst. 2012;104:700–8.
88. Boellaard R, O'Doherty MJ, Weber WA, Mottaghy FM, Lonsdale MN, Stroobants SG, et al. FDG PET and PET/CT: EANM procedure guidelines for tumour PET imaging: version 1.0. Eur J Nucl Med Mol Imaging. 2010;37:181–200.
89. Timmers HJ, Kozupa A, Chen CC, Carrasquillo JA, Ling A, Eisenhofer G, et al. Superiority of fluorodeoxyglucose positron emission tomography to other functional imaging techniques in the evaluation of metastatic SDHB-associated pheochromocytoma and paraganglioma. J Clin Oncol. 2007;25:2262–9.
90. Gabriel M, Decristoforo C, Donnemiller E, Ulmer H, Watfah Rychlinski C, Mather SJ, et al. An intrapatient comparison of 99mTc-EDDA/HYNIC-TOC with 111In-DTPA-octreotide for diagnosis of somatostatin receptor-expressing tumors. J Nucl Med. 2003;44:708–16.
91. Grimes J, Celler A, Birkenfeld B, Shcherbinin S, Listewnik MH, Piwowarska-Bilska H, et al. Patient-specific radiation dosimetry of 99mTc-HYNIC-Tyr3-octreotide in neuroendocrine tumors. J Nucl Med. 2011;52:1474–81.
92. Pacak K, Eisenhofer G, Carrasquillo JA, Chen CC, Li ST, Goldstein DS. 6-[18F]fluorodopamine positron emission tomographic (PET) scanning for diagnostic localization of pheochromocytoma. Hypertension. 2001;38:6–8.
93. Ilias I, Yu J, Carrasquillo JA, Chen CC, Eisenhofer G, Whatley M, et al. Superiority of 6-[18F]-fluorodopamine positron emission tomography versus [131I]-metaiodobenzylguanidine scintigraphy in the localization of metastatic pheochromocytoma. J Clin Endocrinol Metab. 2003;88:4083–7.
94. Mann GN, Link JM, Pham P, Pickett CA, Byrd DR, Kinahan PE, et al. [11C]Metahydroxyephedrine and [18F]fluorodeoxyglucose positron emission tomography improve clinical decision making in suspected pheochromocytoma. Ann Surg Oncol. 2006;13:187–97.
95. Shulkin BL, Wieland DM, Schwaiger M, Thompson NW, Francis IR, Haka MS, et al. PET scanning with hydroxyephedrine: an approach to the localization of pheochromocytoma. J Nucl Med. 1992;33:1125–31.
96. Trampal C, Engler H, Juhlin C, Bergstrom M, Langstrom B. Pheochromocytomas: detection with 11C hydroxyephedrine PET. Radiology. 2004;230:423–8.
97. Franzius C, Hermann K, Weckesser M, Kopka K, Juergens KU, Vormoor J, et al. Whole-body PET/CT with 11C-meta-hydroxyephedrine in tumors of the sympathetic nervous system: feasibility study and comparison with 123I-MIBG SPECT/CT. J Nucl Med. 2006;47:1635–42.
98. Rahbar K, Kies P, Stegger L, Juergens KU, Weckesser M. Discrepancy between glucose metabolism and sympathetic nerve terminals in a patient with metastatic paraganglioma. Eur J Nucl Med Mol Imaging. 2008;35:687.
99. Loc'h C, Mardon K, Valette H, Brutesco C, Merlet P, Syrota A, et al. Preparation and pharmacological characterization of [76Br]-meta-bromobenzylguanidine ([76Br]MBBG). Nucl Med Biol. 1994;21:49–55.
100. Vaidyanathan G, Affleck DJ, Zalutsky MR. Validation of 4-[fluorine-18]fluoro-3-iodobenzylguanidine as a positron-emitting analog of MIBG. J Nucl Med. 1995;36:644–50.
101. Yu M, Bozek J, Lamoy M, Guaraldi M, Silva P, Kagan M, et al. Evaluation of LMI1195, a novel 18F-labeled cardiac neuronal PET imaging agent, in cells and animal models. Circ Cardiovasc Imaging. 2011;4:435–43.
102. Martiniova L, Perera SM, Brouwers FM, Alesci S, Abu-Asab M, Marvelle AF, et al. Increased uptake of [123I]meta-iodobenzylguanidine, [18F]fluorodopamine, and [3H]norepinephrine in mouse pheochromocytoma cells and tumors after treatment with the histone deacetylase inhibitors. Endocr Relat Cancer. 2011;18:143–57.
103. Taieb D, Rubello D, Al-Nahhas A, Calzada M, Marzola MC, Hindie E. Modern PET imaging for paragangliomas: relation to genetic mutations. Eur J Surg Oncol. 2011;37:662–8.
104. Havekes B, King K, Lai EW, Romijn JA, Corssmit EP, Pacak K. New imaging approaches to phaeochromocytomas and paragangliomas. Clin Endocrinol (Oxf). 2010;72:137–45.